Food and Chemical Toxicology 161 (2022) 112841

Contents lists available at ScienceDirect

Food and Chemical Toxicology

journal homepage: www.elsevier.com/locate/foodchemtox

Investigation of the genotoxicity of digested titanium dioxide nanomaterials in human intestinal cells

Adriana Vieira [a], Nádia Vital [a], Dora Rolo [a], Rossana Roque [a], Lídia M. Gonçalves [b], Ana Bettencourt [b], Maria João Silva [a,c], Henriqueta Louro [a,c,*]

[a] Department of Human Genetics, National Institute of Health Dr. Ricardo Jorge (INSA), Avenida Padre Cruz, 1649-016, Lisboa, Portugal
[b] Research Institute for Medicine (iMed.ULisboa), Faculty of Pharmacy, Universidade de Lisboa, 1649-003, Lisbon, Portugal
[c] ToxOmics–Centre for Toxicogenomics and Human Health, NOVA Medical School, Universidade NOVA de Lisboa, Campo dos Mártires da Pátria, 130, 1169-056, Lisboa, Portugal

ARTICLE INFO

Handling Editor: Dr. Jose Luis Domingo

Keywords:
Titanium Dioxide
Nanomaterials
In vitro simulated digestion
Intestinal epithelial cells
Genotoxicity

ABSTRACT

The widespread use of titanium dioxide nanomaterials (TiO_2 NMs) in food and consumer products such as toothpaste or food contact materials, suggests the relevance of human oral exposure to these nanomaterials (NMs) and raises the possibility of adverse effects in the gastrointestinal tract (GIT).

We previously showed that the *in vitro* digestion of TiO_2 NMs may increase their toxicity in intestinal cells. In this work, we analyzed the genotoxicity and the intracellular reactive oxygen species induction by physiologically relevant concentrations of three different TiO_2 NMs (NM-102, NM-103 and NM-105) in Caco-2 and HT29-MTX-E12 intestinal cells, while considering the potential influence of the digestion process in the NMs' physiochemical characteristics. The results evidenced a DNA-damaging effect dependent on the NM, more relevant for the rutile/anatase NM-105, possibly due to its lower hydrodynamic size in the cells medium. In addition, the results of the micronucleus assay suggest effects on chromosomal integrity, an indicator of cancer risk, in the HT29-MTX-E12 cells, for all the tested TiO_2 NMs, especially after the *in vitro* digestion. This work supports the evidence for concerns on the use of TiO_2 NMs as a food additive, recently reported by EFSA, and for their use in applications in consumer products that may drive human exposure through ingestion.

1. Introduction

Titanium dioxide nanomaterials (TiO_2 NMs) are among the nanomaterials (NMs) most frequently applied in industries dealing with toothpaste, pharmaceuticals, coatings, papers, inks, plastics, food products, cosmetics and textile (Waghmode et al., 2019). As food additives, TiO_2 NMs enhance the white color of some products, such as dairy products, pastries, candies, sweets and chewing gums; their use can also improve the flavor of non-white foods like vegetables, nuts, soups, sauces and for clearing beverages like beer, cider and wine (Weir et al., 2012; Winkler et al., 2018). This class of NMs may also be applied in food contact materials (He et al., 2019). Very recently, the application of TiO_2 as a food additive (E171) was considered no longer safe by the European Food Safety Authority, EFSA (EFSA Panel on Food Additives and Flavourings et al., 2021a). Nevertheless, the widespread use of TiO_2 NMs in the pharmaceutical, personal hygiene, or cosmetics industries has been equally described. As such, apart from food products, also dietary supplements, toothpaste, and lipstick, among other products, are sources of nanosized TiO_2 exposure and may contribute to a health risk from exposure to these NMs (Heringa et al., 2016). It is noteworthy that these products are outside the regulation for the food sector.

The wide use of TiO_2 NMs has led to an increased potential for human exposure, and the human internal exposure has already been demonstrated (Heringa et al., 2018). Additionally, a study with the Dutch population, showed that the products contributing most to young children TiO_2 NMs intake were, in fact, toothpaste (contributing to over 57% of the TiO_2 NMs' intake) while in adults the intake was spread over many food products, including raw cow milk samples, possibly originated from the background or indirect sources (Rompelberg et al., 2016). This exposure data reinforces the possibility of adverse effects at

* Corresponding author. Department of Human Genetics, National Institute of Health Dr. Ricardo Jorge (INSA), Avenida Padre Cruz, 1169-056, Lisboa, Portugal.
E-mail addresses: adriana.vieira@insa.min-saude.pt (A. Vieira), nadia.vital@insa.min-saude.pt (N. Vital), dora.rolo@insa.min-saude.pt (D. Rolo), rossana.roque@insa.min-saude.pt (R. Roque), lgoncalves@ff.ulisboa.pt (L.M. Gonçalves), M.Joao.Silva@insa.min-saude.pt (M.J. Silva), henriqueta.louro@insa.min-saude.pt (H. Louro).

https://doi.org/10.1016/j.fct.2022.112841
Received 24 August 2021; Received in revised form 22 December 2021; Accepted 25 January 2022
Available online 31 January 2022

the gastrointestinal tract (GIT). *In vivo* rodent models have been used to investigate such effects upon ingestion, while providing a whole-organism realistic approach that includes the modifications that TiO_2 NMs undergo in the digestion process (Bettini et al., 2017; Bettini and Houdeau, 2014; Murugadoss et al., 2020; Urrutia-Ortega et al., 2016), but the differences in the physiology and uptake of the GIT between humans and rodents may hamper an adequate risk assessment (Sohal et al., 2018a). Therefore, the use of simulated human digestion models provides a valuable early-stage tool for hazard characterization of NMs, as an alternative to animal models. Although the *in vitro* digestion is not specific for NMs, the INFOGEST harmonized method is considered by EFSA as a key approach to be used for NMs after food consumption (EFSA et al., 2021b).

The TiO_2 NMs potential toxicity in the GIT has not been clarified yet, since the results from *in vitro* studies are contradictory (reviewed in EFSA Panel on Food Additives and Flavourings et al., 2021a), many showing some evidence of genotoxicity of TiO_2 NMs in intestinal cells (Dorier et al., 2017; Gerloff et al., 2012; NanoGenoTox, 2013; Schneider et al., 2017; Vila et al., 2018; Zijno et al., 2015). To include the digestion process in the comparative toxicity assessment of ingested TiO_2 NMs, we have previously described the application of the standardized static INFOGEST 2.0 *in vitro* digestion method to three different TiO_2 NMs (NM-102, NM-103 and NM-105). The doses were selected as physiologically relevant for the human intestine following oral intake (Richter et al., 2018; Guo et al., 2017). Interestingly, the hydrodynamic size of NM-105 decreased after digestion and, compared with the pristine form, a more toxic effect occurred in HT29-MTX-E12 cells (Bettencourt et al., 2020). This decreased hydrodynamic size after digestion may have also consequences on its genotoxicity. For further exploring the biological effects of ingested TiO_2 NMs, the objective of the present work was to investigate the genotoxicity of the same TiO_2 NMs in two intestinal cell lines, after undergoing a simulated digestion process, and to relate the outcome to their primary and secondary physicochemical characteristics. Since oxidative stress has been frequently associated with toxicity induced by TiO_2 NMs (Proquin et al., 2017), complementary analysis of reactive oxygen species (ROS) was included in this investigation.

2. Materials and methods

2.1. TiO_2 NMs' physicochemical properties and sample preparation

The three TiO_2 NMs used in this work, NM-102, NM-103 and NM-105, were kindly provided by the Joint Research Centre (JRC, Ispra, Italy) and are considered as international benchmarks (Rasmussen et al., 2014). Their primary physicochemical characteristics were provided by JRC (Rasmussen et al., 2014). With primary sizes between 22 and 30 nm, the three TiO_2 NMs display differences in the crystalline structure, surface area and agglomerate/aggregate sizes. NM-102 and NM-103 comprise anatase and rutile crystalline phases, respectively, whereas NM-105 presents mixed crystallinity of both 81.5% anatase and 18.5% rutile. Furthermore, NM-103 is the only coated NM, comprising a hydrophobic Al-coating (Rasmussen et al., 2014).

A 2.56 mg/mL stock dispersion of each NM was prepared by pre-wetting powder in 0.5% absolute ethanol (96%) followed by the addition of sterile-filtered 0.05 wt % of bovine serum albumin (BSA)-water and dispersion by 16 min of probe sonication of the sample with a 400-Watt Branson Sonifier S-450D (Branson Ultrasonics Corp., Danbury, CT, USA), cooled in an ice-water bath (Jensen et al., 2011). The stock dispersions were immediately used either for the static digestion process (resulting in the digested samples, DIG) or directly (corresponding to the undigested samples) for physicochemical characterization and biological assays, after dilution in cell culture medium.

The human digestion of TiO_2 NMs was mimicked by the use of a static digestion protocol based on the standardized INFOGEST 2.0 *in vitro* digestion method (Brodkorb et al., 2019). After the simulated digestion, TiO_2 NMs samples were diluted in the cell culture medium, to the final concentrations of 0.14, 1.4 and 14 μg/mL of digested NMs for immediate use in the genotoxicity assays.

The characterization of the secondary properties of the NMs in the biological medium using DLS, zeta potential and TEM-EDS, including the effect of simulated GIT medium, was described previously by our group (Bettencourt et al., 2020). Briefly, DLS data showed that after digestion NM-105 has a lower mean size than the pristine one, while no major differences were observed for the other NMs. All undigested and digested NMs showed negative zeta potentials and sizes of the NMs dispersed in culture medium measured by TEM ranged from 20.4 to 25.7 nm (Bettencourt et al., 2020).

2.2. Cell culture and exposure

Two distinct human intestinal cell lines were selected as *in vitro* experimental models, undifferentiated Caco-2 cells and HT29-MTX-E12 cells (ECACC, UK). Undifferentiated cells were used since it is recognized that the mucosa of the small intestine is comprised of both mature differentiated villus enterocytes that are directly exposed to the intestinal lumen and poorly differentiated proliferative enterocytes that reside in the crypts below the luminal surface (P. Greaves, 2007). Both cell lines were maintained in Dulbecco's Modified Eagle Medium (DMEM), supplemented with 1% Amphotericin B (0.25 mg/mL), 1% solution of 10,000 units/mL of penicillin and 10,000 μg/mL of streptomycin, 2.5% HEPES Buffer and 10% or 15% fetal bovine serum (FBS), for HT29-MTX-E12 or Caco-2 cells, respectively. All reagents were obtained from Thermo Fisher (Waltham, MA, USA). The cells were maintained at 37 °C and an atmosphere with 5% CO_2.

The undigested or digested TiO_2 NMs samples were diluted in cell culture medium, to the final concentrations of 0.14, 1.4 and 14 μg/mL. The concentrations were selected based on published works that have considered 0.14 μg/mL as a realistic concentration reaching the human intestine, based on real-life oral exposure (Richter et al., 2018; Guo et al., 2017). In addition, our previous results showed that neither undigested nor digested samples were cytotoxic within the selected concentration range (Bettencourt et al., 2020).

For the comet assay, Caco-2 and HT29-MTX-E12 cells were plated at a density of $7x10^4$ cells per well in 24-well plates and incubated for 24 h before exposure. The exposure medium was added and an exposure period of 24 h was used. The positive control was 5 mM of ethyl methanesulfonate (EMS; Sigma-Aldrich, St. Louis, MO, USA) and it was added 1 h before cell harvesting.

Regarding the CBMN assay, HT29-MTX-E12 cells were plated at a density of $0.5x10^5$ cells per well in 6-well plates and Caco-2 cells were seeded with a density of $1.5x10^5$ cells/mL in each 25 cm^2 flask and both incubated for 24 h before exposure. Mitomycin C (Sigma-Aldrich, St. Louis, MO, USA) was used as a positive control at a final concentration of 0.3 μg/mL.

The solution of BSA-water used to disperse the NMs, as well as the digested BSA-Water (DIG Control), corresponding to the digested negative control (without NM). Three digestion negative controls were used: C1, corresponding to the percentage of the digestion product present in the culture medium for the 0.14 μg/mL NM concentration; C2, for 1.4 μg/mL and C3, for 14 μg/mL.

2.3. Comet assay

Following 24 h of exposure to the NMs, the cells were harvested, and the alkaline comet assay was performed as previously described (Louro et al., 2019). Both the conventional and the Formamidopyrimidine DNA Glycosylase (FPG)-modified versions of the comet assay were performed. The use of DNA repair endonucleases such as FPG allows the detection of DNA oxidation lesions, in addition to single- or double-strand breaks and alkali-labile sites. Briefly, after the exposure, the cell suspension was mixed with 0.8% low melting point agarose (Sigma-Aldrich), placed on microscope slides previously coated with 1%

normal melting point agarose and covered with coverslips. Slides were immersed in lysis solution (NaCl 2.5 M, $Na_2EDTA.2H_2O$ 100 mM, Tris-HCl 10 mM; pH 10; 10% DMSO and 1% Triton-X100), overnight, at 4 °C. Slides were washed with the FPG enzyme reaction buffer (F buffer; HEPES 40 mM, KCl 100 mM, acid EDTA 0.5 mM, BSA 0.2 mg/ml; pH 8). The FPG enzyme (kindly provided by Dr. A. R. Collins, University of Olso, Norway) diluted in F buffer, or the F buffer only, was added to each gel and the slides were incubated for 30 min in a humidified chamber at 37 °C. An incubation for 30 min in electrophoresis buffer (NaOH 0.3 M, $Na_2EDTA.2H_2O$ 1 mM; pH = 13) was followed by electrophoresis at 4 °C for 25 min, 0.8V/cm. Finally, the slides were washed with neutralization buffer (Trizma-base 0.4 M in water, with 9,5%vol HCl 4 M; pH = 7.5) and in MilliQ water. The resulting slides were stained with ethidium bromide (12.5 μg/mL) before analysis under a fluorescence microscope (Leica Dm500, Germany) using the Comet Assay IV image analysis system (Perceptive Instruments, UK). Three replicates from independent experiments per exposure condition were analyzed, with 100 cells scored per treatment condition, in 2 gels. The median of the % DNA in tail from each sample was calculated. The mean ± Standard Deviation (M±SD) of the median value of three independent replicates was used to represent the results. The Net FPG-sensitive sites were determined by subtracting the basal level of DNA migration (% DNA in tail) from the DNA migration in the enzyme-treated slides.

2.4. Cytokinesis-blocked micronucleus assay (CBMN) assay

The cytokinesis-blocked micronucleus assay was performed according to international guidelines with minor changes to overcome the interference of NMs (OECD, 2016; Louro et al., 2016), such as adding cytochalasin-B (Sigma-Aldrich, St. Louis, MO, USA) 24 h after exposure. The cells were incubated for a total of 72 h (HT29-MTX-E12 cells) or 52 h (Caco-2 cells) after the beginning of the exposure to NMs, due to different doubling times and previous preliminary experiments. The resulting Giemsa-stained slides were coded and blind-scored under a bright field microscope (Axioskop 2 Plus, Zeiss, Germany). Micronuclei were scored in, at least, 4000 binucleate cells from two independent cultures. The frequency of micronucleated binucleated cells per 2000 cells (MNBC/1000 BC) was determined. The proportion of mono-, bi- or multinucleated cells was determined in a total of 1000 cells and the cytokinesis-blocked proliferation index (CBPI), as well as the replication Index (RI), was calculated using OECD guideline (OECD, 2016).

2.5. Intracellular reactive oxygen species (ROS) measurement

The intracellular ROS was determined using a well-characterized probe, 2′,7′-Dichlorofluorescein diacetate (H2DCF-DA; Life Technologies, UK) according to a procedure previously described (Silva et al., 2017) with some adaptations. Briefly, Caco-2 and HT29-MTX-E12 cell lines were seeded with equal density in each well of 96-well plates (2×10^4 cells per well) with 100 μL of the cell culture medium per well and incubated for 24 h at 37 °C. Cells were pre-incubated for 30 min with 20 μM of H2DCF-DA, in the dark and at 37 °C. Then the probe solution was removed, and a fresh medium was added containing the different samples to be tested (NM-102, NM-103, NM-105, solution of BSA and digested NM-102, NM-103, NM-105 and BSA) at three final concentrations of 0.14, 1.4 and 14 μg/mL, in three replicates. Hydrogen peroxide solution (250 μM) was used as a positive control for the induction of ROS in cells and cell culture medium alone as a negative control. Cells were incubated in presence of the treatments for 1 and 24 h at 37 °C. The DCF levels were determined at excitation 485 nm and emission 520 nm wavelengths using a fluorescence microplate reader (FLUOstar BMGLabtech, Ortenberg, Germany). Data from three independent experiments were reported as mean relative ROS level expressed as fold-change compared to ROS level in respective controls (fluorescence of exposed cells/fluorescence of unexposed control from the same experiment conditions).

2.6. Determination of H_2O_2 production

ROS-Glo™ H_2O_2 Assay kit, from Promega Corp. (Madison, WI, USA), was used to measure the level of hydrogen peroxide (H_2O_2), one type of ROS, directly in cell culture, using the non-lytic procedure, according to the manufacturer's instructions, with minor modifications, as follow. Briefly, 24 h before the exposure treatment with the NMs, cells were seeded with equal density in each well of 96- well plates (2×10^4 cells per well). After overnight incubation, the cell medium was replaced by the exposure medium. After 18 h, H_20_2 substrate solution was added (25 μM), and incubation proceeded until 24 h. At the end of the treatment, 50 μL of medium from each sample well was combined with 50 μL of ROS-Glo™ Detection Solution in a separate opaque white 96-well plate and plates were incubated for 20min at room temperature, protected from the light. The luminescence signal from the ROS-Glo™ Assay (relative luminescent units, RLU) was measured using a plate reading luminometer (GloMax® 96 Luminometer). The results are expressed as relative to the negative control (BSA-water without digestion) in both Caco-2 and HT29-MTX-E12 cells.

Concomitant negative and positive control was used. The negative control used was the test compound vehicle (BSA-Water), mimicking the highest concentration used with NMs (14 μg/mL; C3) and processed as described above for the NMs. As a positive control for ROS generation, 50 μM of Menadione (Sigma) was selected, as suggested by the manufacturer. The cells were incubated with the positive control for 2 h, in the presence of 25 μM H_2O_2 substrate solution.

2.7. Statistical analysis

The statistical analysis of the results was performed using IBM SPSS Statistics 26 (Armonk, NY, USA) or Prism software (6.01, GraphPad, San Diego, CA, USA). Fisher's exact test was applied to compare the frequency of micronucleated cells of NM-treated and vehicle-treated cultures. CBPI, RI and DNA damage were analyzed using one-way ANOVA and *post-hoc* tests. In addition, Student's *t*-test was used to compare the digested and undigested treatment conditions at the same concentration, as well as the results with and without the FPG enzyme and ROS levels. For comparing the generation of H_20_2 between samples relatively to control one-way ANOVA followed by Dunnett's post hoc test for multiple comparisons was performed, provided that the data followed a normal distribution, to compare multiple treatments relatively to control. Otherwise, non-parametric tests were applied, such as Kruskal-Wallis to compare differences between the tested concentrations and the negative control. Differences with a p-value lower than 0.05 were considered statistically significant.

3. Results

3.1. DNA damage induced by digested TiO_2 NMs

The results of the quantification of DNA damage in both types of human intestinal cells, assessed using the conventional and FPG-modified comet assays after 24 h of exposure, are presented in Figs. 1 and 2. The Net FPG-sensitive sites are presented in Table 1 for both cell lines.

In Caco-2 cells, a significant increase in DNA damage was observed 24 h after exposure to 14 μg/mL of digested NM-102 and NM-103 (Fig. 1A and B), when compared to the respective undigested counterparts ($p = 0.037$, $p = 0.001$; Student's *t*-test). In the FPG-comet assay, there was an increase in DNA oxidation damage after 1.4 μg/mL of digested NM-102 (Fig. 1D, $p = 0.018$, Student's *t*-test) and after 14 μg/mL of digested NM-105 (Fig. 1F, $p = 0.010$) compared to the undigested sample.

Significant differences were detected in DNA damage induced by 24 h exposure to the digested NM-103 and digested NM-105 in relation to their respective negative controls ($p = 0.015$ and $p = 0.046$, One-Way

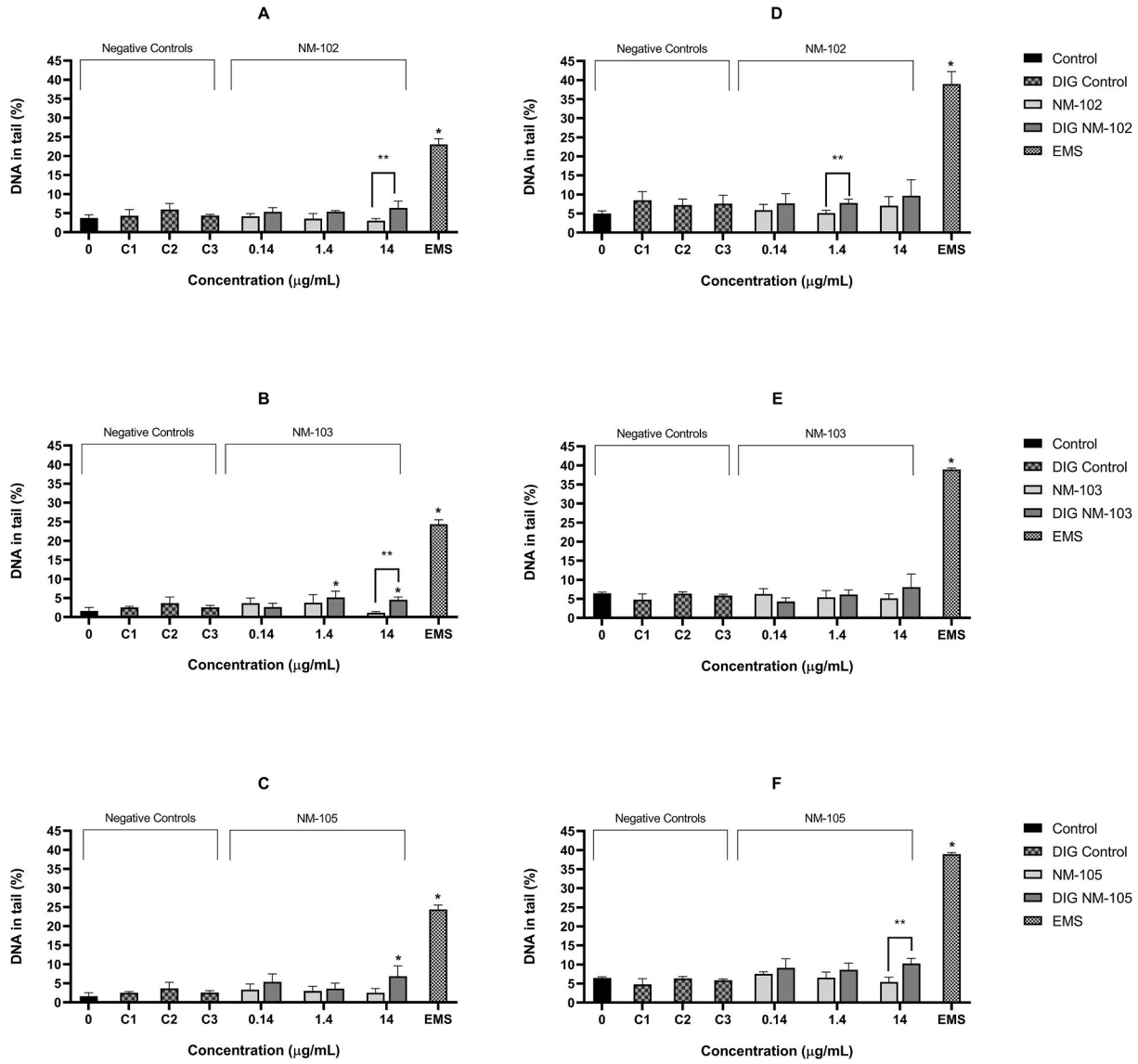

Fig. 1. Results of the conventional (A–C) or FPG-comet assay (D–F) in Caco-2 cells, after 24 h exposure to undigested and digested (DIG NM) TiO_2 NMs: NM-102 **(A, D)**, NM-103 **(B, E)** and NM-105 **(C, F)**. 0 - negative control (medium containing BSA-waster); C1, C2, C3 - digested negative controls for 0.14, 1.4 and 14 μg/mL of NM, respectively; EMS positive control, 5 mM. The results are represented as the mean % of DNA in tail (±SD) of three independent replicates. * - Significantly different from the respective negative or digested negative control ($p < 0.05$, One-Way ANOVA and Post-hoc tests). ** - Digested NM sample is significantly different from the undigested NM sample, at the same concentration ($p < 0.05$, Student's *t*-test).

ANOVA). DNA damage induced by the digested NM-103 (1.4 and 14 μg/mL) and digested NM-105, 14 μg/mL, was significantly higher than the respective negative control ($p = 0.031$, $p = 0.011$ and $p = 0.034$ Student's *t*-test). However, the values related to digested NM-103 are contained within the 95% confidence interval of the distribution of our historical negative control data, with a lower bound of 4.038 and an upper bound of 5.861 in % DNA in tail, while the value of DIG NM-105 is outside of this interval, being more relevant.

The Net-FPG sensitive sites did not reveal significant increases in oxidative damage after digestion either in Caco-2 or in HT29-MTX-E12 cells (Table 1).

The levels of DNA damage measured after a short exposure for 3 h to each undigested or digested NM did not show significant differences over the respective controls, in any of the cell lines. Likewise, no significant differences in DNA damage were observed between each digested and the corresponding undigested NM sample (results not shown).

Additionally, no significant differences were observed in DNA damage in both cell types (Figs. 1 and 2), when exposed to several concentrations of the digested negative controls (C1–C3) compared to the negative control, BSA water ($p > 0.05$, Student's t-test). On the other hand, positive controls exhibited a significant increase in DNA damage and oxidative lesions, confirming the sensitivity of the assay to detect DNA single- and double-stranded breaks.

Regarding HT29-MTX-E12 cells (Fig. 2), a significant difference was observed when comparing the results from cells exposed to digested NM-103 samples at 1.4 μg/mL compared to undigested counterparts, both in conventional and FPG-comet assays ($p = 0.0054$ and $p = 0.012$, respectively; Student's *t*-test). Moreover, digested NM-105 induced an increase in the percentage of DNA in tail at the concentration of 0.14 μg/mL, in the absence of FPG ($p = 0.044$) and at 14 μg/mL with the enzyme ($p = 0.014$), compared to the undigested sample at the same concentration. Also, in HT29-MTX-E12 cells the highest concentration of the digested NM-105 led to a mild significant increase in the level of DNA damage when compared to its negative control, in the conventional and FPG-modified comet assays ($p = 0.028$ and $p = 0.025$, respectively;

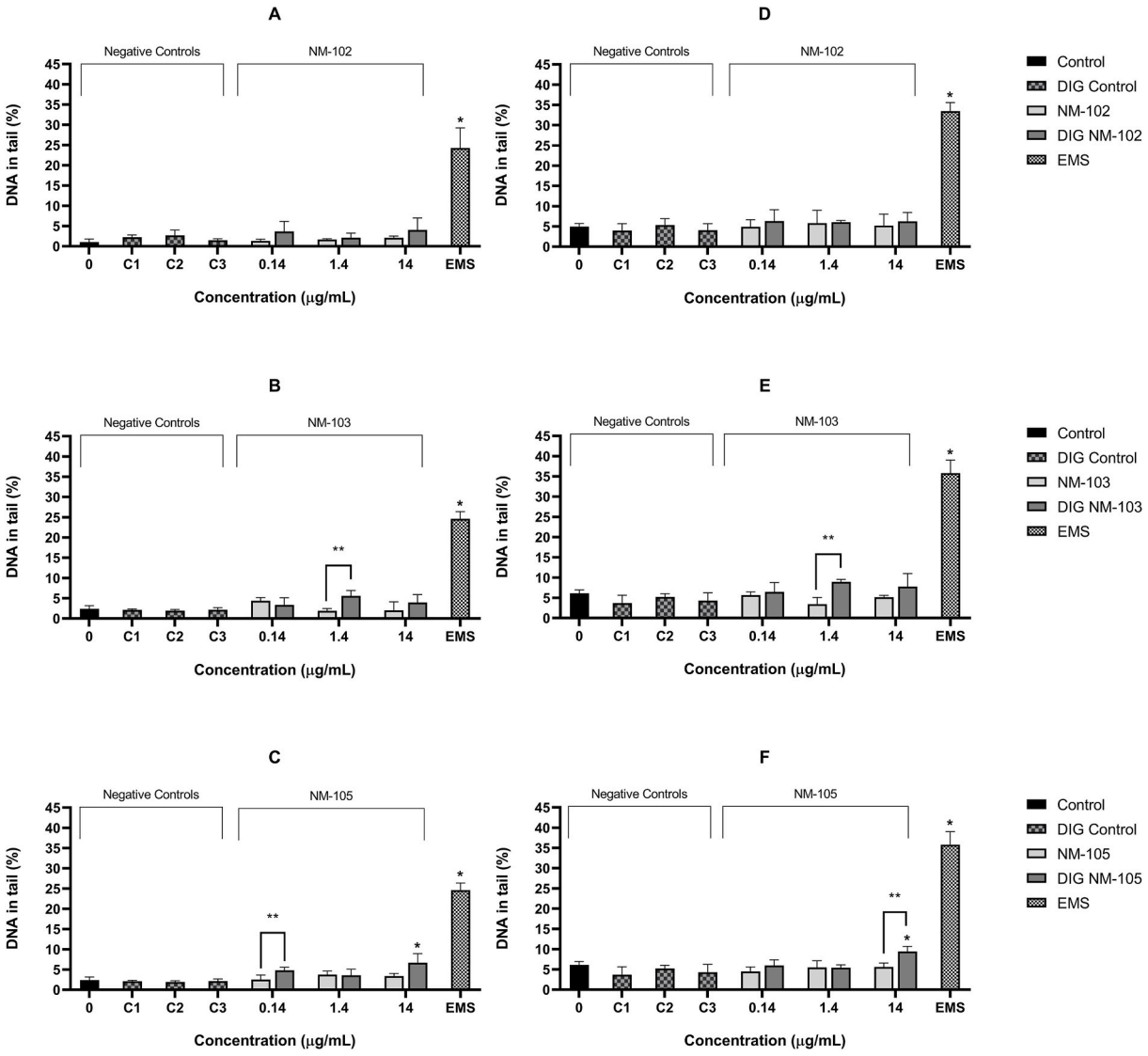

Fig. 2. Results of conventional (A–C) or FPG-comet assay (D–F) in HT29-MTX-E12 cells, after 24 h exposure to undigested and digested (DIG NM) TiO_2 NMs: NM-102 **(A, D)**, NM-103 **(B, E)** and NM-105 **(C, F)**. 0 - negative control (medium containing BSA-waster); C1, C2, C3 - digested negative controls for 0.14, 1.4 and 14 μg/mL of NM, respectively; EMS positive control, 5 mM. The results are represented as the mean % of DNA in tail (±SD) of three independent replicates. * - Significantly different from the respective negative or digested negative control ($p < 0.05$, One-Way ANOVA and Post-hoc tests). ** - Digested NM sample is significantly different from the undigested NM sample, at the same concentration ($p < 0.05$, Student's *t*-test).

Tuckey *post-hoc* test). The significant values observed for DIG NM-105 were outside the 95% confidence interval of the distribution of the historical negative control data, ranging from 1.673 to 2.314% DNA in tail (in the conventional comet assay) or from 4.094 to 5.331% in the FPG-combined comet assay, suggesting that the increase in DNA oxidation damage is a relevant finding after digestion of NM-105 as compared to undigested sample, an effect seen also in Caco-2.

The OECD criteria for the identification of a positive response in a given genotoxicity test can be used to aid in the interpretation of the results obtained (OECD, 2017). A clear positive result is considered if three criteria are met, namely a statistically significant increase at least for one concentration, dose-response and the relevant result is outside the distribution of the appropriate historical negative control data (OECD, 2017). In addition, the outcome can be considered equivocal if a statistically significant increase in one or more of the concentrations was obtained, but the relevant results were contained inside the distribution of the historical negative control data (NanoGenoTox Joint Action, 2013). Applying the criteria described to the comet assay results, only digested NM-105, at the highest concentration considered, potentially induces an increase in DNA damage in both intestinal cell lines, in the absence of the FPG enzyme, or an increase in DNA oxidation damage in HT29-MTX-E12 cells, considering the assay with FPG.

3.2. Chromosomal damage induced by digested TiO_2 NMs

The results of the CBMN assay in Caco-2 and HT29-MTX-E12 cells exposed to undigested and digested TiO_2 NMs are presented in Figs. 3 and 4.

In Caco-2 cells (Fig. 3), the comparison between digested and undigested NM samples at the same concentration revealed a statistically significant difference in the frequency of micronuclei after 14 μg/mL of digested NM-102 and NM-103 ($p = 5.6 \times 10^{-8}$ and $p = 1.9 \times 10^{-4}$, Fisher's exact test). However, it should be noted that the highest concentration of the digested negative control (C3) was able to induce a significant increase in the MNBC/1000 BC, as compared to the negative control without digestion ($p < 0.05$, Fisher's exact test). Having this background genotoxicity in mind, since negative controls of similar concentrations were used, the comparisons with the respective negative

Table 1
Net-FPG sites determined in the comet assay, 24 h after exposure.

Net FPG-sensitive sites (mean ± SD)	Caco-2 Cells				HT-29-MTX-E12 cells	
	NM-102	NM-103	NM-105	NM-102	NM-103	NM-105
0	1.25 ± 0.66	4.82 ± 0.70		3.94 ± 0.01	3.75 ± 1.12	
DIG C1	2.21 ± 2.16	2.26 ± 1.41		1.74 ± 1.13	1.58 ± 1.40	
DIG C2	0.75 ± 0.23	2.68 ± 1.66		2.69 ± 0.49	3.32 ± 0.64	
DIG C3	3.19 ± 1.84	3.31 ± 0.21		2.58 ± 1.02	2.14 ± 1.45	
0.14	1.71 ± 1.17	2.62 ± 0.24*	4.25 ± 0.85	3.61 ± 1.42	1,28 ± 0,69	1,95 ± 0,64
1.4	1.58 ± 1.10	1.64 ± 1.01*	3.56 ± 2.01	4.16 ± 2.62	1,56 ± 0,91	1,73 ± 0,73
14	4.07 ± 1.88	4.01 ± 0.71	2.88 ± 1.20	3.16 ± 2.68	3,15 ± 1,69	2,21 ± 1,31
DIG 0.14	2.35 ± 1.78	1.68 ± 0.29	3.74 ± 1.42	2.66 ± 0.31	3,14 ± 2,38	1,16 ± 0,6
DIG 1.4	2.40 ± 0.85	0.98 ± 0.53	5.02 ± 0.63	3.94 ± 1.02	3,38 ± 1,28	1,84 ± 0,87
DIG 14	2.21 ± 2.16	3.53 ± 2.54	3.40 ± 2.76	2.24 ± 1.01	3,82 ± 2,02	2,74 ± 1,75
EMS	15.99 ± 1.62*	14.58 ± 1.23*		9.18 ± 2.34*	11.16 ± 2.04*	

0 - negative control (BSA-waster); C1, C2, C3 - digested negative controls for 0.14, 1.4 and 14 μg/mL of NM, respectively; * Significantly different from corresponding negative control, $p < 0.05$ Student's *t*-test. When comparing digested with undigested samples, no significant differences were observed ($p > 0.05$ Student's *t*-test). SD- Standard deviation.

controls of the digested negative control were possible and did not reveal any significant increase of the micronucleus frequency that could be related to digested NMs. A significant increase in the micronucleus frequency was observed only after exposure to 14 μg/mL of undigested NM-105, as compared to the negative control ($p = 0.009$, Fisher's exact test), while other undigested or digested NMs did not elicit significant changes in Caco-2 cells, compared to respective negative controls.

In HT29-MTX-E12 cells (Fig. 4), the digested NM-102 induced an increase in the micronucleus frequency when compared with undigested samples, at the concentrations of 1.4 and 14 μg/mL ($p = 0.023$ and $p = 0.000016$, Fisher's exact test). Likewise, digested NM-103 also increased significantly the frequency of micronucleated cells at the highest concentration ($p = 0.001$, Fisher's exact test), while it produced a significant decrease at the lowest concentration tested ($p = 0.04$, Fisher's exact test). However, as observed in Caco-2 cells, the induction of micronucleus by the digestion controls, at the highest concentration, weakens the evidence at the concentration of 14 μg/mL. Nevertheless, in HT29-MTX-E12, a significant increase was observed in the micronuclei frequencies following exposure to all concentrations of the undigested and digested NM-102, as compared to respective negative controls ($p < 0.05$, Fisher's exact test). This increase can be attributed to NM-102, either undigested or digested. In addition, it was observed an increase in MNBC/1000 BC frequency in cells exposed to the concentrations of 0.14 and 1.4 μg/mL of the undigested and digested NM-103, as compared to the negative control ($p = 0.000037$ and $p = 0.016$, respectively; Fisher's exact test). The undigested NM-105 induced also an increase in the frequency micronucleated cells after exposure to all concentrations, as compared to negative controls, but only the concentration of 0.14 μg/mL of digested NM-105 induced a statistically significant increase in the frequency of micronuclei ($p = 0.0004$, Fisher's exact test). Therefore, considering the OECD criteria for the identification of a positive response (OECD, 2017), we identify NM-102, NM-103 and NM-105 as potentially genotoxic in HT29-MTX-E12 cells under the tested conditions, in general triggering increased chromosomal damage after digestion simulation, while no such effect occurs in Caco-2 cells.

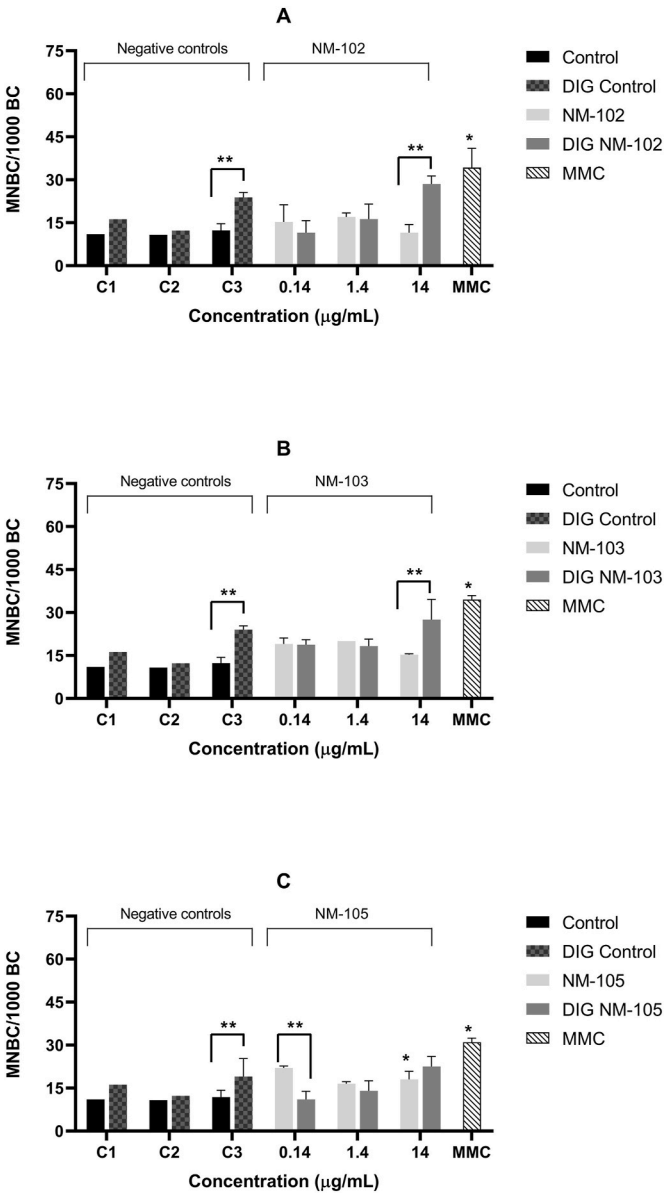

Fig. 3. Results of the CBMN assay in Caco-2 cells, after 52 h of exposure to undigested and digested (DIG NM) TiO_2 NMs: NM-102 **(A)**, NM-103 **(B)** and NM-105 **(C)**. C1, C2, C3 - digested negative controls for 0.14, 1.4 and 14 μg/mL of NM, respectively; MMC- positive control, 0.3 μg/mL. The results are represented as mean MNBC/1000 BC ± SD of two independent replicates (n = 2). * - Significantly different from the respective negative control, i.e. comparable concentration of BSA water for undigested NM samples and digested negative control (DIG Control) for digested NM samples ($p < 0.05$, Fisher's Exact test). ** - The digested sample is significantly different from the undigested sample, at the same concentration ($p < 0.05$, Fisher's Exact test). MNBC/1000 BC – Micronucleated binucleated cells per 1000 binucleated cells.

3.3. Reactive oxygen species induced by digested TiO2 NMs

The intracellular production of ROS after exposure of Caco-2 and HT29-MTX-E12 cells to the different undigested and digested TiO_2 NMs was first evaluated using the H2DCF-DA reagent (Figs. 5 and 6). In both cell lines, after 1 h or 24 h of exposure to the undigested samples, no significant increase was observed compared with the control culture medium. Only for the highest tested concentrations, a 1.5- to 2-fold increase in ROS levels was observed for all digested, as compared to undigested samples, at the same concentration ($p < 0.05$, Student's *t*-test). However, this increase was apparently due to the digestion

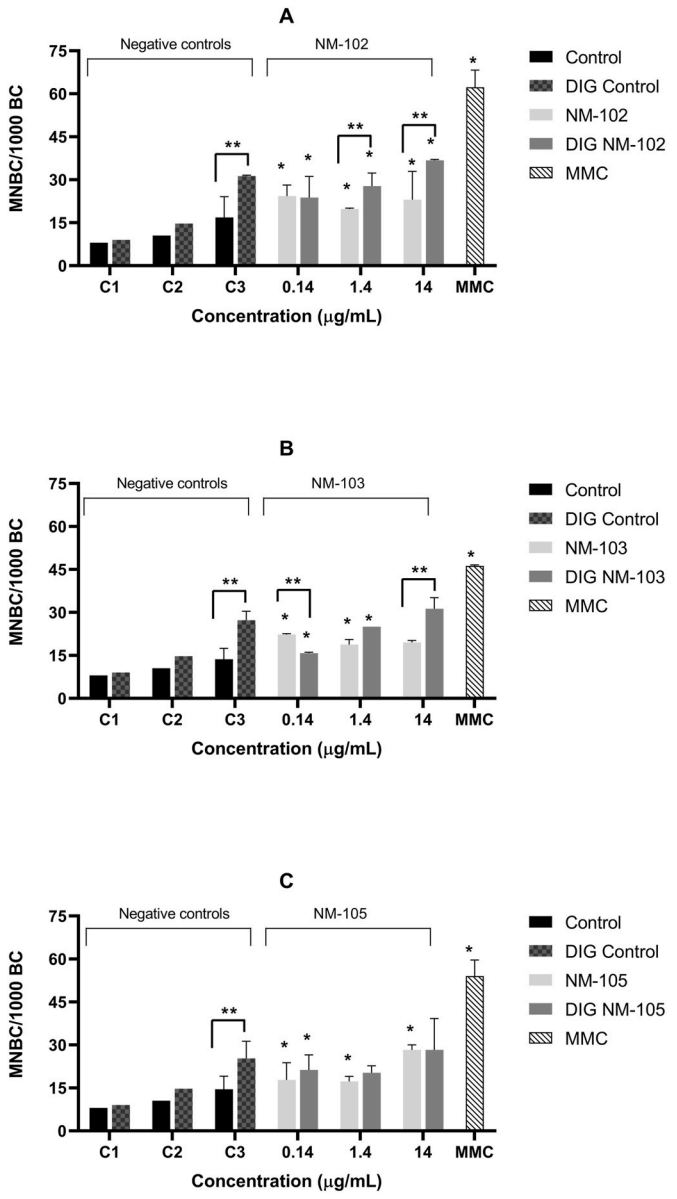

Fig. 4. Results of the CBMN assay in HT29-MTX-E12 cells, after 72 h of exposure to undigested and digested (DIG NM) TiO_2 NMs: NM-102 **(A)**, NM-103 **(B)** and NM-105 **(C)**. C1, C2, C3 - digested negative controls for 0.14, 1.4 and 14 μg/mL of NM, respectively; MMC- positive control, 0.3 μg/mL. The results are represented as mean MNBC/1000 BC ± SD of two independent replicates (n = 2). * - Significantly different from the respective negative control, i.e. comparable concentration of BSA water for undigested NM samples and digested negative control (DIG Control) for digested NM samples ($p < 0.05$, Fisher's Exact test). ** - The digested sample is significantly different from the undigested sample, at the same concentration ($p < 0.05$, Fisher's Exact test). MNBC/1000 BC – Micronucleated binucleated cells per 1000 binucleated cells.

medium itself, since it was independent of the presence of the NM. The effect of the digestion medium as an inducer of ROS was eliminated after 10 times dilution, but no induction of ROS was observed that could be attributed to the TiO_2 NMs, either directly or following digestion, after 1 or 24 h of exposure to the tested concentrations.

Figure 7 presents data on H_20_2 generation, measured in cell medium using the luminescent ROS-Glo™ H_2O_2 Assay. In general, it was also observed that the digested negative control *per se*, at the highest concentration, was able to induce H_20_2 production, although the increase was significant only for Caco-2 cells.

While the positive control induced a major increase in peroxide production, in both cells, the NMs, either digested or not, did not show clear increases, despite small but significantly increases in Caco-2 cells exposed to the highest dose tested for all digested nanomaterials (Fig. 7-A, B, C). Even though, this effect was possibly due to the digested negative control itself and not to the NMs. In HT29-MTX-E12 cells, a slight decrease of H_20_2 generation was observed after exposure to 14 μg/mL of digested TiO_2 NMs. In the absence of cells, the digested BSA-water displayed an increase H_20_2 generation at the highest dose, which was also significative for both digested NM-102 and NM-103 (data not shown). In general, the ROS-Glo™ H_2O_2 Assay seemed less sensitive than the H2DCF-DA method, possibly due to the specificity to detect H_2O_2 instead of several types of ROS such as hydroxyl, peroxyl and other reactive oxygen species (ROS) that can be detected within the cell using H2DCF-DA. Furthermore, the latter detects intracellular ROS, while H_2O_2 measurements (Fig. 7) refer to extracellular levels.

4. Discussion

In this work, we aimed to investigate the genotoxicity of three TiO_2 NMs, NM-102, NM-103 and NM-105 after undergoing an *in vitro* digestion process, that we previously showed that can influence the secondary physicochemical characteristics of NM-105 in intestinal cell medium (Bettencourt et al., 2020). Comet assay results suggest that digested NM-105, at the highest concentration considered, induces an increase in DNA damage in both intestinal cell lines, in the absence of the FPG enzyme, or an increase in DNA oxidation damage in HT29-MTX-E12 cells, in the assay with FPG. Conversely, NM-102, NM-103 and NM-105 are potentially genotoxic in HT29-MTX-E12 cells, leading to chromosomal damage, an effect that is maintained by the digested NMs, while no effect occurs in Caco-2 cells. Complementary ROS analysis did not reveal oxidative stress induction, either directly or after the digestion process.

The absence of ROS induction in cells exposed to the TiO_2 NMs, directly or after the digestion process, is in line with the low level of oxidative DNA damage observed in the FPG-comet assay, suggesting that at physiologically relevant concentrations for the human intestine (Richter et al., 2018; Guo et al., 2017), these effects are of no concern. Many studies have reported ROS induction, but for higher TiO_2 concentrations (Dorier et al., 2019), or in repeated exposure conditions (Dorier et al., 2017), while for lower doses most studies reported negative effects (Abbott Chalew and Schwab, 2013; de Angelis et al., 2013; Jalili et al., 2018; Jensen et al., 2019). For example, intracellular ROS generation was not found, either in undifferentiated Caco-2 cells following exposure to 0.125–125 μg/mL E171, for 3 h (Jensen et al., 2019) or in differentiated Caco-2 cells, after a 3 h or 24 h exposure to 0–256 μg/mL of TiO_2 NM rutile hydrophobic (JRC benchmark NM-103, 25 nm) and rutile hydrophilic forms (JRC benchmark NM-104, 25 nm) (Jalili et al., 2018). Conversely, an increase in ROS generation was observed in undifferentiated Caco-2 cell cultures, following exposure to 100 μg/mL and 200 μg/mL of two digested anatases with different sizes (99 and 26 nm) for 24 h, but did not affect differentiated Caco-2 cells (Song et al., 2015). Interestingly, ROS generation was inhibited in medium comprising 0.05% BSA in two human colon cancer cells lines (Caco-2 and/or HCT116), as measured by electron spin resonance spectroscopy, following 24 h exposure to 0.143 and 1.43 μg/cm^2 (equivalent to 1 and 10 μg/mL) of E171, and TiO_2 NM (10–30 nm) (Proquin et al., 2017). The authors suggested a scavenging or inhibitory effect by the protein corona which may prevent ROS formation by inhibiting the contact between the particle surface and ROS precursors. In this study, because cells exposure medium contained proteins from FBS and BSA (dispersion medium) the occurrence of such ROS inhibitory effect cannot be excluded. However, the digested negative control without any NM was able to increase the ROS levels at the highest concentration and this background effect may be explained by the composition of the solution used for the digestion of the NMs (Brodkorb et al., 2019). This oxidant effect of the digested negative control, that

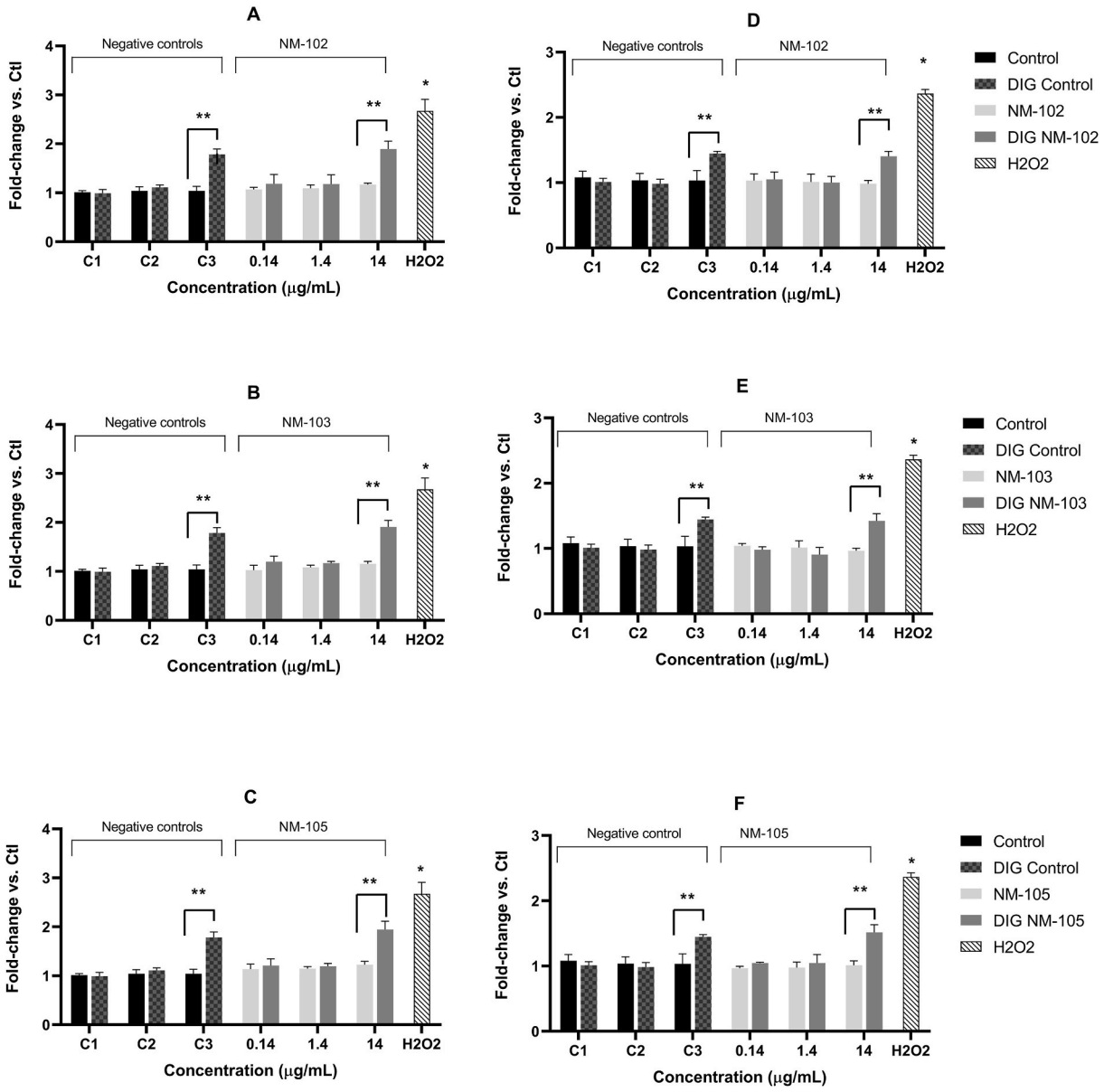

Fig. 5. Intracellular ROS content in Caco-2 (A,B,C) and HT29-MTX-E12 (D,E,F) for 1 h at 0.14, 1.4 and 14 μg/mL of undigested and digested (Dig NM) TiO_2 NMs: NM-102 (A,D), NM-103 (B,E) and NM-105 (C,F). ROS level is expressed as fold-change compared to ROS level in control cells. (Mean ± standard deviation, n = 3). * - Significantly different from the respective negative culture medium control ($p < 0.05$). ** - The digested sample is significantly different from the undigested sample, at the same concentration ($p < 0.05$).

was visible in both cell lines at the highest concentration, may be a result of several factors, such as the inclusion of a high content of bile salts in the simulated digestion protocol, particularly in the small intestinal phase, that was already reported to be a problem in other digestion protocols (DeLoid et al., 2017). Consistently, a background effect was observed in the micronucleus assay at this concentration, but no effect was detected by the comet assay or FPG-comet assay. Possibly, the effect of the digested negative control leading to an increased background was only detectable after the longer exposure period that was used for micronucleus assay (52–72 h) as compared to the comet assay (24 h). Such background genotoxicity at the highest digested negative control concentration cannot be attributed to potential toxicity, since no relevant decreases of the CBPI and RI (calculated in the MN assay), was observed in both cell lines (data not shown). In agreement, previous results showed no cytotoxicity after 24 h of exposure to the same NMs (Bettencourt et al., 2020).

Other mechanisms, apart from the possibility of ROS induction, may explain the genotoxicity of TiO_2 NMs observed in intestinal cells through the comet and MN assay, such as the direct interaction with the DNA molecule, interfering with the replication process and/or cell functioning (Magdolenova et al., 2014; Gurr et al., 2005). Previously, our group observed the decrease in the NM-105 hydrodynamic size following the *in vitro* digestion simulation process, assessed by DLS (Bettencourt et al., 2020), maybe due to the action of proteolytic enzymes used in the simulated digestion process In this study we observed that the highest concentration the digested NM-105 was able to induce DNA strand breaks in both cell lines while the other NMs were not. Smaller NMs present a larger surface area and consequently, the potential for a higher reactivity in biological systems (Dorier et al., 2017). Indeed, smaller NMs have an increased possibility of uptake by cells, and of moving through the cell compartments, reaching eventually the nucleus. As a result, these particles may interact with the DNA molecule, leading to genotoxic damage (Magdolenova et al., 2014).

There are some reports in the literature that used the *in vitro* comet

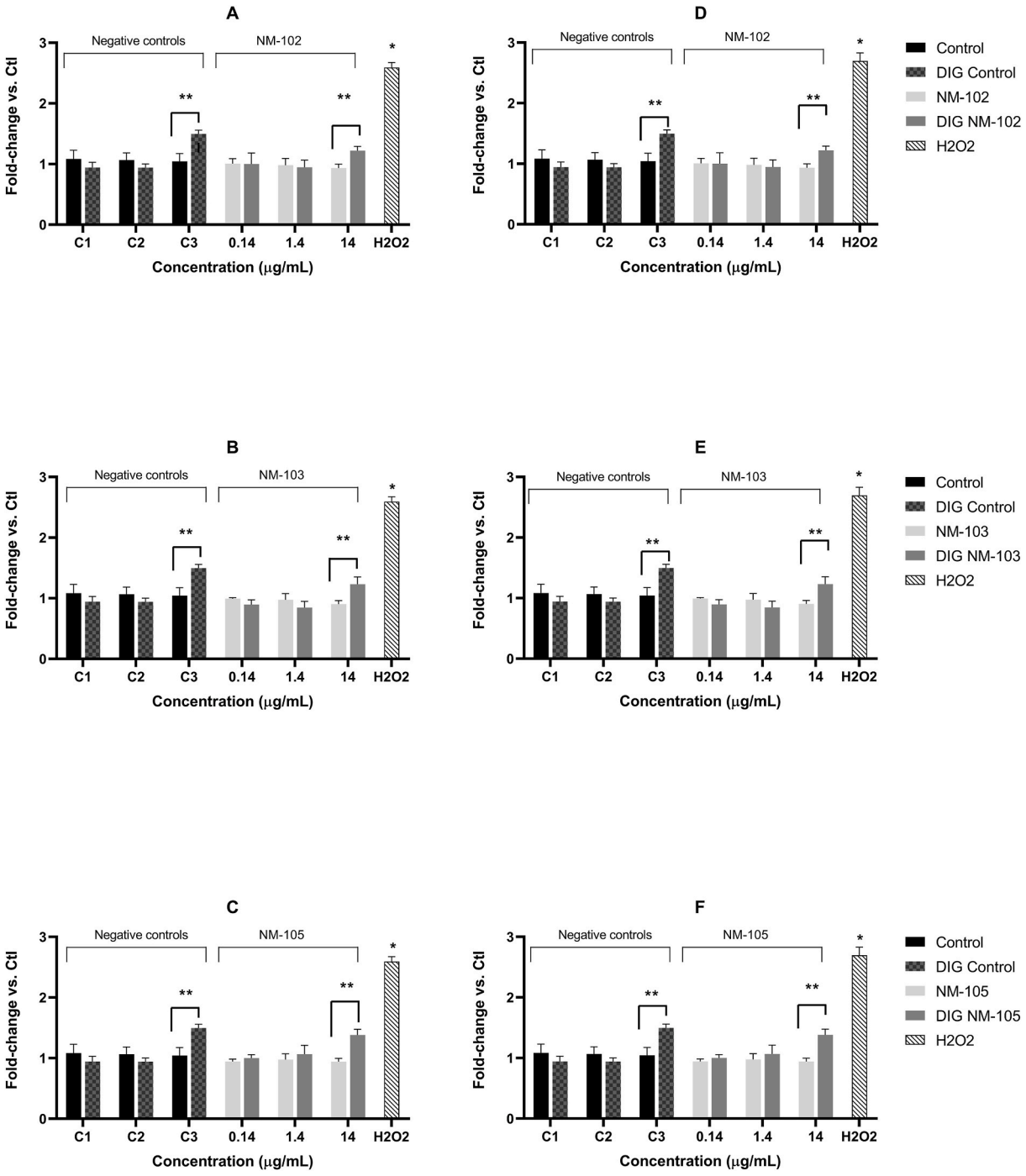

Fig. 6. Intracellular ROS content in Caco-2 (A,B,C) and HT29-MTX-E12 (D,E,F) for 24 h at 0.14, 1.4 and 14 μg/mL of undigested and digested (Dig NM) TiO_2 NMs: NM-102 (A,D), NM-103 (B,E) and NM-105 (C,F). ROS level is expressed as fold-change compared to ROS level in control cells. (Mean ± standard deviation, n = 3). * - Significantly different from the respective negative culture medium control ($p < 0.05$). ** - The digested sample is significantly different from the undigested sample, at the same concentration ($p < 0.05$).

assay in the genotoxicity testing of TiO_2 NMs concerning intestinal cells. The majority of the available results are contradictory, which might be related to the different physicochemical properties of the tested NMs (i.e., size, shape, crystalline phase), as well as distinct experimental conditions (including the exposure period and the concentration range of NMs) (NanoGenoTox Joint Action, 2013). In agreement with our findings of negative results for NM-102 and NM-103 and weak positive results for NM-105, no increase in the DNA strand break level was detected in Caco-2 cells after a 3- or 24 h treatments with 1.2–80 μg/cm^2 concentrations of two rutile TiO_2 NMs, NM-103 and NM-104 (Jalili et al., 2018). Another report using NM-103 (9, 28, 85, 128 and 256 μg/mL), also did not show DNA damage in Caco-2 cells following 3 h or 24 h of exposure, with the conventional and FPG-modified comet assays (Dorier et al., 2015). While negative results were reported for 3 h exposure to NM-102, NM-103, NM-105 positive results were, however, reported for these NMs upon 24 h exposure to a dose up to 256 μg/mL (NanoGenoTox, 2013). Only one report was found in HT29 cells (a different clone from HT29-MTX-E12), where the exposure to 8 and 10 μg/mL of anatase/rutile TiO_2 NM (21 nm) for 24 h led to an increase in the DNA strand break level and oxidative lesions (Schneider et al., 2017). In one

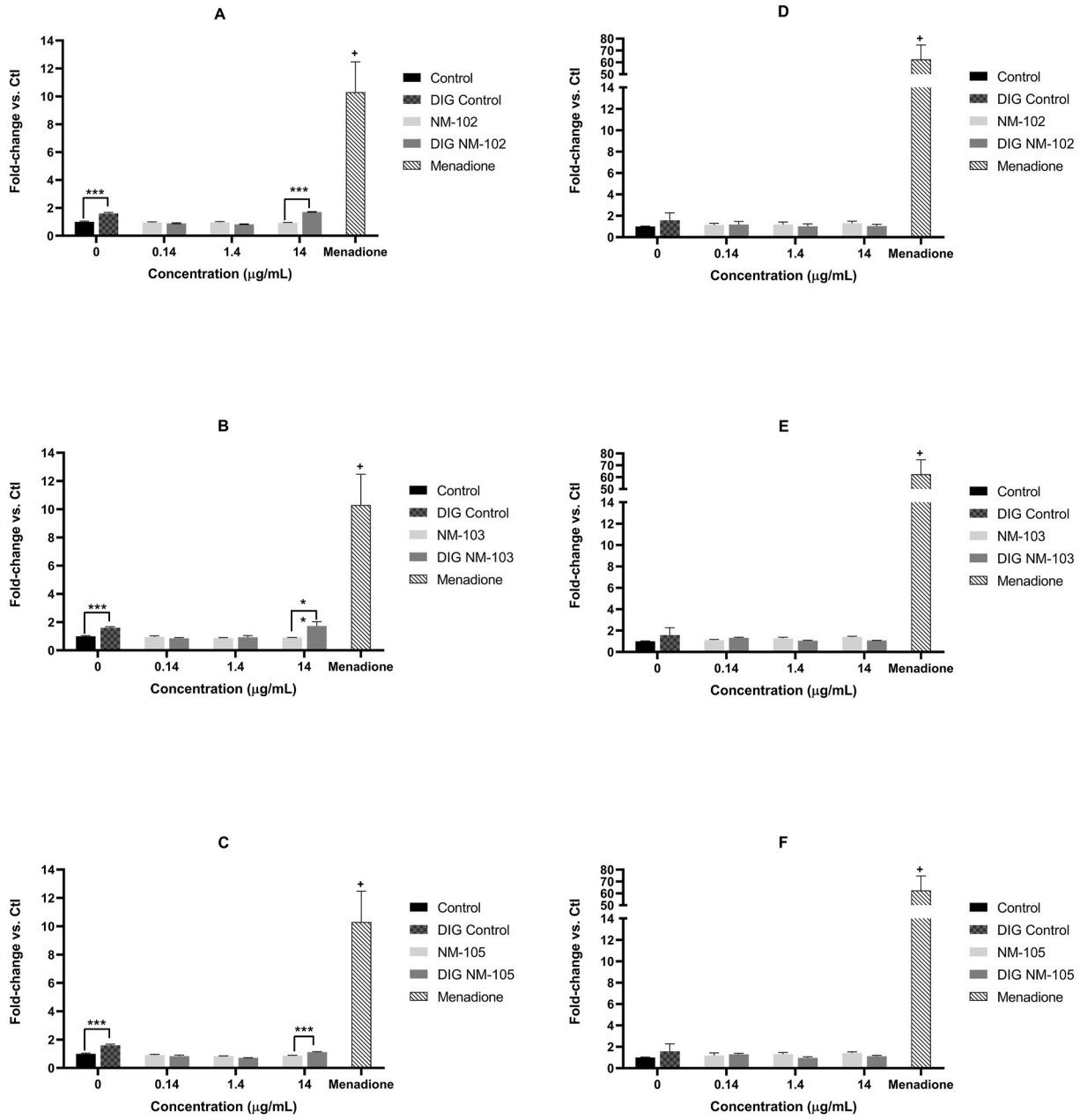

Fig. 7. H_20_2 production in Caco-2 (A,B,C) and HT29-MTX-E12 (D,E,F) medium after 24 h exposure to different concentrations of undigested and digested (DIG) NM102 (A), NM103 (B) and NM105(C), for 24 h. H_20_2 level is expressed as fold-change compared to H_20_2 level in BSA-Water (undigested). (Mean ± standard deviation, n = 3). * statistically significant difference in H_20_2 of digested concentrations relative to undigested concentrations (*$p < 0.01$; **$p < 0.001$; ***$p < 0.0001$);+denote a statistically significant difference in H_20_2 production of positive control (menadione, 50 μM, for 2 h exposure) relative to undigested BSA-Water (equivalent to concentration 14).

report, Caco-2 and HT29-MTX co-cultures were exposed to 50 μg/mL of NM-105 or E171 and did not show genotoxic effects in the comet assay (Dorier et al., 2019).

Concerning chromosomal damage, previous reports on the micronucleus assay in Caco-2 cells suggested negative results after 52 h of exposure to NM-102, NM-103, NM-104 and NM-105 (NanoGenoTox, 2013), in line with our results. Using 1–20 μg/cm^2 of anatase TiO_2 NM, negative results were also reported in Caco-2 exposed for 6 h and 24 h; similar negative results were reported for NM-103 and NM-104 tested in differentiated Caco-2 cells (Jalili et al., 2018; Zijno et al., 2015). In the human colon adenocarcinoma (HCT116) cell line, a positive micronucleus induction was observed after 5–50 μg/cm^2 of E171 (Proquin et al., 2017). It is noteworthy that no studies were found in the literature about the genotoxicity of these NMs in HT29-MTX-E12 cells. Thus, the present indication of potential genotoxicity of the three TiO_2 NMs in HT29-MTX-E12 cells, more relevant after digestion, provides a novel finding relevant for their hazard and risk assessment. Micronuclei may originate from chromosome breakage or loss during mitosis (Fenech et al., 2011). The aneugenic effect is frequently the result of DNA replication block due to adducts formation, e.g., oxidation adducts, whereas the aneugenic effect results mainly from the interaction of the substance with the mitotic fibers and its consequent disruption. We may hypothesize that, because no prominent oxidation DNA damage was observed and thus no adducts are probably formed between the NMs and the DNA molecule, a disruption of the mitotic fibers due to the nanoparticles internalization by cells is more likely to have occurred.

Comparing the two cell lines here used as models of human intestinal cells, the present results suggest that HT29-MTX-E12 cells show higher

sensitivity than Caco-2 cells to the chromosomal damage induced by the TiO_2 NMs irrespective of its form, while similar sensitivity is observed in the comet and ROS assays. Although both cell lines are derived from intestinal cancer tissue and were used in their undifferentiated status, Caco-2 can differentiate to absorptive enterocyte cells, while the HT29-MTX can differentiate to mucus-secreting cells. Therefore, they have different characteristics according to their physiological functions that may explain their different sensitivity, e.g., different uptake capacity. Further studies on nano-cellular interactions in each cell line, namely concerning cellular uptake and trafficking are underway to investigate this difference and underlying mechanisms.

5. Conclusion

Despite many studies reporting the assessment of DNA or chromosomal damage in several types of intestinal cells after exposure to TiO_2 NMs (reviewed in EFSA Panel on Food Additives and Flavourings et al., 2021a), to our knowledge, no study used an *in vitro* digestion method on these NMs for the investigation of genotoxicity of ingested TiO_2 NMs.

Considering the importance of the digestion process in the physiochemical characteristics of the ingested NMs, and the influence of the biological medium, in this work we have analyzed the genotoxicity of physiologically relevant concentrations of three different TiO_2 NMs in intestinal cells. We observed a DNA-damaging effect that was dependent on the NM, being more relevant for the rutile/anatase, NM-105, possibly due to the lower hydrodynamic size that this NM harbors in intestinal moiety (Bettencourt et al., 2020). The link of this positive effect with the decrease in the hydrodynamic size of NM-105 following *in vitro* digestion suggests a mechanistic rationale for the observed effect that will be further confirmed by uptake studies. In addition, the cytokinesis-blocked micronucleus assay, which is considered as an indicator of chromosomal integrity disruption, may raise further concerns for the cancer risk of the three TiO_2 NMs, in the intestinal tissue upon oral exposure and NMs digestion. Thus, the *in vitro* digestion process emerges as a screening tool for improving the insights of nano-genotoxicity assessment, a step closer to *in vivo* models. This is pivotal for the risk assessment of TiO_2 NMs used in food products, because they will pass though that process before reaching the GIT where they can exert adverse effects. Future *in vivo* studies can be designed to complement the findings on the several forms of ingested TiO_2 NMs.

Finally, this work is in line with the evidence for concerns on the use of E171 as a food additive (EFSA Panel on Food Additives and Flavourings et al., 2021a), and also for the use of TiO_2 NMs in other applications which may drive human exposure through ingestion.

CRediT authorship contribution statement

Adriana Vieira: Investigation, Methodology, Writing – original draft, Writing – review & editing, All authors have read and agreed to the published version of the manuscript. **Nádia Vital:** Investigation, Methodology, Writing – review & editing, All authors have read and agreed to the published version of the manuscript. **Dora Rolo:** Investigation, Methodology, Writing – review & editing, All authors have read and agreed to the published version of the manuscript. **Rossana Roque:** Methodology, All authors have read and agreed to the published version of the manuscript. **Lídia M. Gonçalves:** Investigation, All authors have read and agreed to the published version of the manuscript. **Ana Bettencourt:** Investigation, All authors have read and agreed to the published version of the manuscript. **Maria João Silva:** Funding acquisition, Investigation, Writing – review & editing, All authors have read and agreed to the published version of the manuscript. **Henriqueta Louro:** Conceptualization, Funding acquisition, Investigation, Writing – original draft, Writing – review & editing.

Declaration of competing interest

The authors declare that they have no known competing financial interests or personal relationships that could have appeared to influence the work reported in this paper.

Acknowledgments

This work was funded by national funds through the FCT - Foundation for Science and Technology, I.P., under the project PTDC/SAU-PUB/29481/2017. Research co-funded by UIDB/00009/2020; UIDP/00009/2020 (Centre for Toxicogenomics and Human Health – ToxOmics, FCT- Foundation for Science and Technology). NV holds a FCT PhD Scholarship grant (2020.07168.BD). iMed.ULisboa (UIDB/04138/2020 and UIDP/04138/2020) principal investigator grants CEECIND/03143/2017 (L. M. Gonçalves).

The authors thank all the support from the colleagues Paula Alvito, Carla Martins and Ricardo Assunção (Food Safety Department, INSA, Lisbon, Portugal) as well from all INGESTnano team members.

References

Abbott Chalew, T.E., Schwab, K.J., 2013. Toxicity of commercially available engineered nanoparticles to Caco-2 and SW480 human intestinal epithelial cells. Cell Biol. Toxicol. 29 (2), 101–116. https://doi.org/10.1007/s10565-013-9241-6.

Bettencourt, A., Gonçalves, L.M., Gramacho, A.C., Vieira, A., Rolo, D., Martins, C., Assunção, R., Alvito, P., Silva, M.J., Louro, H., 2020. Analysis of the characteristics and cytotoxicity of titanium dioxide nanomaterials following simulated in vitro digestion. Nanomaterials 10 (8), 1516. https://doi.org/10.3390/nano10081516.

Bettini, S., Boutet-Robinet, E., Cartier, C., Coméra, C., Gaultier, E., Dupuy, J., Naud, N., Taché, S., Grysan, P., Reguer, S., Thieriet, N., Réfrégiers, M., Thiaudière, D., Cravedi, J.P., Carrière, M., Audinot, J.N., Pierre, F.H., Guzylack-Piriou, L., Houdeau, E., 2017. Food-grade TiO2 impairs intestinal and systemic immune homeostasis, initiates preneoplastic lesions and promotes aberrant crypt development in the rat colon. Sci. Rep. 20 (7), 40373. https://doi.org/10.1038/srep40373.

Bettini, S., Houdeau, E., 2014. Exposition orale aux nanoparticules de dioxyde de titane (TiO2): du franchissement de l'épithélium buccal et intestinal au devenir et aux effets dans l'organisme. Biologie Aujourd'hui 208 (2), 167–175. https://doi.org/10.1051/jbio/20140022.

Brodkorb, A., Egger, L., Alminger, M., Recio, I., 2019. INFOGEST static in vitro simulation of gastrointestinal food digestion. Nat. Protoc. https://doi.org/10.1038/s41596-018-0119-1.

de Angelis, I., Barone, F., Zijno, A., Bizzarri, L., Russo, M.T., Pozzi, R., Franchini, F., Giudetti, G., Uboldi, C., Ponti, J., Rossi, F., de Berardis, B., 2013. Comparative study of ZnO and TiO2 nanoparticles: physicochemical characterisation and toxicological effects on human colon carcinoma cells. Nanotoxicology 7 (8), 1361–1372. https://doi.org/10.3109/17435390.2012.741724.

DeLoid, G.M., Wang, Y., Kapronezai, K., Lorente, L.R., Zhang, R., Pyrgiotakis, G., Konduru, N.V., Ericsson, M., White, J.C., De La Torre-Roche, R., Xiao, H., McClements, D.J., Demokritou, P., 2017. An integrated methodology for assessing the impact of food matrix and gastrointestinal effects on the biokinetics and cellular toxicity of ingested engineered nanomaterials. Part. Fibre Toxicol. 14 (1), 1–17. https://doi.org/10.1186/s12989-017-0221-5.

Dorier, M., Brun, E., Veronesi, G., Barreau, F., Pernet-Gallay, K., Desvergne, C., Rabilloud, T., Carapito, C., Herlin-Boime, N., Carrière, M., 2015. Impact of anatase and rutile titanium dioxide nanoparticles on uptake carriers and efflux pumps in Caco-2 gut epithelial cells. Nanoscale 7 (16), 7352–7360. https://doi.org/10.1039/c5nr00505a.

Dorier, M., Béal, D., Marie-Desvergne, C., Dubosson, M., Barreau, F., Houdeau, E., Herlin-Boime, N., Carriere, M., 2017. Continuous in vitro exposure of intestinal epithelial cells to E171 food additive causes oxidative stress, inducing oxidation of DNA bases but no endoplasmic reticulum stress. Nanotoxicology. https://doi.org/10.1080/17435390.2017.1349203.

Dorier, Marie, Tisseyre, C., Dussert, F., Béal, D., Arnal, M.E., Douki, T., Valdiglesias, V., Laffon, B., Fraga, S., Brandão, F., Herlin-Boime, N., Barreau, F., Rabilloud, T., Carriere, M., 2019. Toxicological impact of acute exposure to E171 food additive and TiO2 nanoparticles on a co-culture of Caco-2 and HT29-MTX intestinal cells. Mutat. Res. Genet. Toxicol. Environ. Mutagen 845. https://doi.org/10.1016/j.mrgentox.2018.11.004.

EFSA Panel on Food Additives and Flavourings, Younes, M., Aquilina, G., Castle, L., Engel, K.H., Fowler, P., Frutos Fernandez, M.J., Fürst, P., Gundert-Remy, U., Gürtler, R., Husøy, T., Manco, M., Mennes, W., Moldeus, P., Passamonti, S., Shah, R., Waalkens-Berendse, n I., Wölfle, D., Corsini, E., Cubadda, F., De Groot, D., FitzGerald, R., Gunnare, S., Gutleb, A.C., Mast, J., Mortensen, A., Oomen, A., Piersma, A., Plichta, V., Ulbrich, B., Van Loveren, H., Benford, D., Bignami, M., Bolognesi, C., Crebelli, R., Dusinska, M., Marcon, F., Nielsen, E., Schlatter, J., Vleminckx, C., Barmaz, S., Carfí, M., Civitella, C., Giarola, A., Rincon, A.M., Serafimova, R., Smeraldi, C., Tarazona, J., Tard, A., Wright, M., 2021a. Safety

assessment of titanium dioxide (E171) as a food additive. EFSA J. 19 (5), e06585 https://doi.org/10.2903/j.efsa.2021.6585.
EFSA, S.C., More, S., Bampidis, V., Benford, D., Bragard, C., Halldorsson, T., Hernández-Jerez, A., Hougaard Bennekou, S., Koutsoumanis, K., Lambré, C., Machera, K., Naegeli, H., Nielsen, S., Schlatter, J., Schrenk, D., Silano Deceased, V., Turck, D., Younes, M., Castenmiller, J., Chaudhry, Q., Cubadda, F., Franz, R., Gott, D., Mast, J., Mortensen, A., Oomen, A.G., Weigel, S., Barthelemy, E., Rincon, A., Tarazona, J., Schoonjans, R., 2021b. Guidance on risk assessment of nanomaterials to be applied in the food and feed chain: human and animal health. EFSA J. 19 (8), e06768 https://doi.org/10.2903/j.efsa.2021.6768.
Fenech, M., Kirsch-Volders, M., Natarajan, A.T., Surralles, J., Crott, J.W., Parry, J., Norppa, H., Eastmond, D.A., Tucker, J.D., Thomas, P., 2011 Jan. Molecular mechanisms of micronucleus, nucleoplasmic bridge and nuclear bud formation in mammalian and human cells. Mutagenesis 26 (1), 125–132. https://doi.org/10.1093/mutage/geq052.
Gerloff, K., Fenoglio, I., Carella, E., Kolling, J., Albrecht, C., Boots, A.W., Förster, I., Schins, R.P.F., 2012. Distinctive toxicity of TiO2 rutile/anatase mixed phase nanoparticles on Caco-2 cells. Chem. Res. Toxicol. https://doi.org/10.1021/tx200334k.
Greaves, P., 2007. Histopathology of Preclinical Toxicity Studies. Elsevier-Academic Press, London, 9780080471303.
Guo, Z., Martucci, N.J., Moreno-Olivas, F., Tako, E., Mahler, G.J., 2017. Titanium dioxide nanoparticle ingestion alters nutrient absorption in an in vitro model of the small intestine. NanoImpact 5, 70–82. https://doi.org/10.1016/j.impact.2017.01.002.
Gurr, J.R., Wang, A.S.S., Chen, C.H., Jan, K.Y., 2005. Ultrafine titanium dioxide particles in the absence of photoactivation can induce oxidative damage to human bronchial epithelial cells. Toxicology 213 (1–2), 66–73. https://doi.org/10.1016/j.tox.2005.05.007.
He, X., Deng, H., Hwang, H. min, 2019. The current application of nanotechnology in food and agriculture. J. Food Drug Anal. 27 (1), 1–21. https://doi.org/10.1016/j.jfda.2018.12.002.
Heringa, M.B., Geraets, L., van Eijkeren, J.C.H., Vandebriel, R.J., de Jong, W.H., Oomen, A.G., 2016. Risk assessment of titanium dioxide nanoparticles via oral exposure, including toxicokinetic considerations. Nanotoxicology. https://doi.org/10.1080/17435390.2016.1238113.
Heringa, M.B., Peters, R.J.B., Bleys, R.L.A.W., van der Lee, M.K., Tromp, P.C., van Kesteren, P.C.E., van Eijkeren, J.C.H., Undas, A.K., Oomen, A.G., Bouwmeester, H., 2018. Detection of titanium particles in human liver and spleen and possible health implications. Part. Fibre Toxicol. 15 (1), 15. https://doi.org/10.1186/s12989-018-0251-7.
Jalili, P., Gueniche, N., Lanceleur, R., Burel, A., Lavault, M.-T., Sieg, H., Böhmert, L., Meyer, T., Krause, B.-C., Lampen, A., Estrela-Lopis, I., Laux, P., Luch, A., Hogeveen, K., Fessard, V., 2018. Investigation of the in vitro genotoxicity of two rutile TiO2 nanomaterials in human intestinal and hepatic cells and evaluation of their interference with toxicity assays. NanoImpact 11, 69–81. https://doi.org/10.1016/J.IMPACT.2018.02.004.
Jensen, D.M., Løhr, M., Sheykhzade, M., Lykkesfeldt, J., Wils, R.S., Loft, S., Møller, P., 2019. Telomere length and genotoxicity in the lung of rats following intragastric exposure to food-grade titanium dioxide and vegetable carbon particles. Mutagenesis 34 (2), 203–214. https://doi.org/10.1093/mutage/gez003.
Jensen, K.A., Kembouche, Y., Christiansen, E., Jacobsen, N.R., Wallin, H., Guiot, C., Spalla, O., Witschger, O., 2011. Final Protocol for Producing Suitable Manufactured Nanomaterial Exposure Media. www.nanogenotox.eu.
Louro, H., Pinhão, M., Santos, J., Tavares, A., Vital, N., Silva, M.J., 2016. Evaluation of the cytotoxic and genotoxic effects of benchmark multi-walled carbon nanotubes in relation to their physicochemical properties. Toxicol. Lett. 262, 123–134. https://doi.org/10.1016/j.toxlet.2016.09.016.
Louro, H., Saruga, A., Santos, J., Pinhão, M., Silva, M.J., 2019. Biological impact of metal nanomaterials in relation to their physicochemical characteristics. Toxicol. Vitro 56, 172–183. https://doi.org/10.1016/j.tiv.2019.01.018.
Magdolenova, Z., Collins, A., Kumar, A., Dhawan, A., Stone, V., Dusinska, M., 2014. Mechanisms of genotoxicity. A review of in vitro and in vivo studies with engineered nanoparticles. Nanotoxicology 8 (3), 233–278. https://doi.org/10.3109/17435390.2013.773464.
Murugadoss, S., Brassinne, F., Sebaihi, N., Petry, J., Cokic, S.M., van Landuyt, K.L., Godderis, L., Mast, J., Lison, D., Hoet, P.H., van den Brule, S., 2020. Agglomeration of titanium dioxide nanoparticles increases toxicological responses in vitro and in vivo. https://doi.org/10.1186/s12989-020-00341-7.
NanoGenoTox, 2013. NANOGENOTOX Final Report. Facilitating the Safety Evaluation of Manufactured Nanomaterials by Characterising Their Potential Genotoxic Hazard, 60. Nanogenotox. Available at: https://www.anses.fr/en/system/files/nanogenotox_final_report.pdf.
OECD, 2016. Oecd guideline for the testing OF chemicals: 487. In: Vitro Mammalian Cell Micronucleus Test. Organisation for Economic Co-operation and Development Publishing, July, 29. https://doi.org/10.1017/CBO9781107415324.004.
OECD, 2017. Overview of the Set of OECD Genetic Toxicology Test Guidelines and Updates Performed in 2014- 2015.
Proquin, H., Rodríguez-Ibarra, C., Moonen, C.G.J., Urrutia Ortega, I.M., Briedé, J.J., de Kok, T.M., van Loveren, H., Chirino, Y.I., 2017. Titanium dioxide food additive (E171) induces ROS formation and genotoxicity: contribution of micro and nano-sized fractions. Mutagenesis 32 (1), 139–149. https://doi.org/10.1093/mutage/gew051.
Rasmussen, K., Mast, J., Temmerman, P.-J. De, et al., 2014. Titanium dioxide, NM-100, NM-101, NM-102, NM-103, NM-104, NM-105: characterisation and physico-chemical properties. In: Science and Policy Report by the Joint Research Centre of the European Commission. Publications Office of the European Union. https://doi.org/10.2788/79554.
Richter, J.W., Shull, G.M., Fountain, J.H., Guo, Z., Musselman, L.P., Fiumera, A.C., Mahler, G.J., 2018. Titanium dioxide nanoparticle exposure alters metabolic homeostasis in a cell culture model of the intestinal epithelium and Drosophila melanogaster. Nanotoxicology 12 (5), 390–406. https://doi.org/10.1080/17435390.2018.1457189.
Rompelberg, C., Heringa, M.B., van Donkersgoed, G., Drijvers, J., Roos, A., Westenbrink, S., Peters, R., van Bemmel, G., Brand, W., Oomen, A.G., 2016. Oral intake of added titanium dioxide and its nanofraction from food products, food supplements and toothpaste by the Dutch population. Nanotoxicology 10 (10), 1404–1414. https://doi.org/10.1080/17435390.2016.1222457.
Schneider, T., Westermann, M., Glei, M., 2017. In vitro uptake and toxicity studies of metal nanoparticles and metal oxide nanoparticles in human HT29 cells. Arch. Toxicol. 91 (11), 3517–3527. https://doi.org/10.1007/s00204-017-1976-z.
Silva, M.M., Calado, R., Marto, J., Bettencourt, A., Almeida, A.J., Gonçalves, L.M.D., 2017. Chitosan nanoparticles as a mucoadhesive drug delivery system for ocular administration. Mar. Drugs 15 (12). https://doi.org/10.3390/MD15120370.
Sohal, I.S., O'Fallon, K.S., Gaines, P., Demokritou, P., Bello, D., 2018. Ingested engineered nanomaterials: state of science in nanotoxicity testing and future research needs. In: Particle and Fibre Toxicology. https://doi.org/10.1186/s12989-018-0265-1.
Song, Z.M., Chen, N., Liu, J.H., Tang, H., Deng, X., Xi, W.S., Han, K., Cao, A., Liu, Y., Wang, H., 2015. Biological effect of food additive titanium dioxide nanoparticles on intestine: an in vitro study. J. Appl. Toxicol. 35 (10), 1169–1178. https://doi.org/10.1002/jat.3171.
Urrutia-Ortega, I.M., Garduño-Balderas, L.G., Delgado-Buenrostro, N.L., Freyre-Fonseca, V., Flores-Flores, J.O., González-Robles, A., Pedraza-Chaverri, J., Hernández-Pando, R., Rodríguez-Sosa, M., León-Cabrera, S., Terrazas, L.I., van Loveren, H., Chirino, Y.I., 2016. Food-grade titanium dioxide exposure exacerbates tumor formation in colitis associated cancer model. Food Chem. Toxicol. https://doi.org/10.1016/j.fct.2016.04.014.
Vila, L., García-Rodríguez, A., Marcos, R., Hernández, A., 2018. Titanium dioxide nanoparticles translocate through differentiated Caco-2 cell monolayers, without disrupting the barrier functionality or inducing genotoxic damage. J. Appl. Toxicol. https://doi.org/10.1002/jat.3630.
Waghmode, M.S., Gunjal, A.B., Mulla, J.A., Patil, N.N., Nawani, N.N., 2019. Studies on the titanium dioxide nanoparticles: biosynthesis, applications and remediation. SN Appl. Sci. 1 (4), 1–9. https://doi.org/10.1007/s42452-019-0337-3.
Weir, A., Westerhoff, P., Fabricius, L., Hristovski, K., Von Goetz, N., 2012. Titanium dioxide nanoparticles in food and personal care products. Environ. Sci. Technol. 46 (4), 2242–2250. https://doi.org/10.1021/es204168d.
Winkler, H.C., Notter, T., Meyer, U., Naegeli, H., 2018. Critical review of the safety assessment of titanium dioxide additives in food. J. Nanobiotechnol. https://doi.org/10.1186/s12951-018-0376-8.
Zijno, A., de Angelis, I., de Berardis, B., Andreoli, C., Russo, M.T., Pietraforte, D., Scorza, G., Degan, P., Ponti, J., Rossi, F., Barone, F., 2015. Different mechanisms are involved in oxidative DNA damage and genotoxicity induction by ZnO and TiO_2 nanoparticles in human colon carcinoma cells. Toxicol. Vitro. https://doi.org/10.1016/j.tiv.2015.06.009.